

## A low cost vision based localization system using fiducial markers<sup>\*</sup>

Alan Mutka<sup>\*</sup> Damjan Miklic<sup>\*</sup> Ivica Draganjac<sup>\*</sup>  
Stjepan Bogdan<sup>\*</sup>

<sup>\*</sup> Faculty of Electrical Engineering and Computing, University of  
Zagreb, Zagreb, Croatia; (e-mail: {alan.mutka, damjan.miklic,  
ivica.draganjac, stjepan.bogdan}@fer.hr)

**Abstract:** This paper investigates a mobile robot self-localization system based on fiducial markers which are placed on the ceiling. Recently there have been many articles related to path planning and coordination of mobile agents within an unknown environment. These algorithms demand dedicated (and often expensive) hardware that is capable of handling complex tasks in real time. In this paper, we have explored the possibility to realize an inexpensive and simple navigation system, based on passive fiducial markers, which are able to guide an autonomous mobile robot along a predefined path. Fiducial markers provide not only improved performance in runtime, but also much better identification and localization. Marker design based on circle shape is presented. Using a low-cost webcam and appropriate marker detection algorithm three features are determined: robot position, new movement direction and marker ID. Experimental results are presented at the end of the paper.

**Keywords:**

Localization; Sensing; Sensor integration and perception; Autonomus vehicle navigation, guidance and control.

### 1. INTRODUCTION

Image processing has become one of the major building blocks of localization and navigation systems for autonomous mobile robots. In the last decade a lot of approaches to localization and navigation have been presented, many of them based on fiducial markers or on unconstrained images. Working with unconstrained images is a quite challenging task, due to complex and computationally demanding algorithms. Recently there have been many articles related to path planning and coordination of mobile agents within an unknown environment. Usually image processing algorithms play an essential role in gathering structural properties of such environments [S. Se, 2002][Chen Zhichao, 2006]. These algorithms demand dedicated (and often expensive) hardware that is capable of handling complex tasks in a real time. Indoor robot localization could be based on active and/or passive markers. Active markers are usually used with simple hardware because they can be easily traced with special sensors. As an example, in [Heesung Chae and Cho, 2006] the infrared sensors are used for localization. Although the proposed approach is robust with respect to illumination conditions, the problem is that infrared beam has wide range, so an additional camera should be used for more precise positioning. In [K. Yoon and Kweon, 2001] a fast landmark tracking and localization algorithm for mobile robot self-localization is presented

using simple artificial landmark detection based on color histogram. The landmark model, consisting of symmetric and repetitive color patches, produces color histograms that are invariant under the geometric and photometric distortions. Authors in [S. Panziery, 2001] presented a low cost vision localization system based on ceiling lamps detection. The algorithm is focused on identifying lamps on the ceiling as natural landmarks. The main benefit is the fact that the proposed method does not require additional markers. Active markers offer several advantages. For example, solutions based on active markers are not time and computationally demanding and markers are easier to locate. However, the main disadvantage is related to the power supply. Each marker needs a power supply which complicates its installation and maintenance. On the other hand, passive markers are cheaper and easy to install but they are much harder to detect. That is a reason why passive markers should be chosen carefully. The main features that differ a passive marker from the surroundings are contrast and shape; the contrast must be as high as possible, and shape has to be unlike other shapes in the nearby area. Generally, circular markers are used since they provide more robust location information than for example square-shaped markers [Andrew C. Rice and Beresford, 2006].

Fiducial markers are predominantly exploited in Augmented Reality (AR) [Rekimoto and Ayatsuka, 2000] where they are used as advanced barcodes for labeling the objects and gathering information from the surroundings. The most popular toolkit for building Marker-based Vision systems is Cantag [A.C. Rice, 2006], an open source

<sup>\*</sup> This work has been supported by the Ministry of Science, Education and Sports of the Republic of Croatia within technology project TP 44-5 "Autonomous mobile platform for cleaning and surveillance".

software that can identify and accurately locate printed markers in three dimensions. Cantag is a sophisticated framework which utilizes very complex image processing algorithms. Fiducial marker employed in Cantag contains up to 147 bits of information. In mobile robot navigation systems, less complex markers can provide enough information for robot localization and path planning.

In this paper we have explored the possibility to realize an inexpensive and simple navigation system, based on visual feedback, which is able to guide an autonomous mobile robot on a predefined path. Low cost embedded platform hardware [KoreBot, 2007] based on Intel Xscale 400MHz processor is used. The intention is to add the proposed navigation system to the existing commercial manually driven cleaning vehicles, to turn them into automatic ones. The paper describes a visual feedback indoor control system based on the passive visual markers placed on the ceiling. Visual markers contain information about a direction angle marker and ID number. Off the shelf webcam, mounted on the top of a mobile robot SHREC (System for Human Replacement in Economical Cleaning), captures RGB images of the ceiling. Once the robot detects the marker, it identifies marker's features and determines a new direction of its movement.

The paper is organized as follows. In section 2 we define the marker design. In section 3 the image processing algorithm is presented, while in section 4 marker information extraction is described. Section 5 is dedicated to the implementation of localization algorithm executed at the mobile robot. Finally, section 6 presents ideas for the future work.

## 2. PASSIVE MARKER DESIGN

When practical implementation of autonomous navigation systems is considered, operating with fiducial markers is much better than operating with unconstrained images [Andrew C. Rice and Beresford, 2006]. Fiducial markers provide not only improved performance at runtime, but also much better identification and localization. The set of fiducial markers proposed in this paper are presented in Fig. 1.

As mentioned before, circular markers provide more robust localization than square-shaped markers. Moreover, image processing algorithms that handle circular markers are simpler than square detecting algorithms. The fiducial marker developed in our lab (LARICS) contains two circles, one inside the other in order to improve the marker detection in parametric space, as described later. The line outside the circles is used to determine marker's orientation. Three lines positioned inside the circle are coding lines which provide a unique marker ID.

Indoor robot localization is obtained using LARICS markers placed on the ceiling. A marker layout is predefined and the position of each marker is defined in world coordinates. The image resolution of a low cost webcam mounted on the mobile platform is 360x296 pixels. The distance from the camera to the ceiling is 3 meters with camera view angle of 30°. The radius of outer circle is determined with respect to the camera resolution and the distance from the ceiling. The resolution of 2 pixel/cm at 360x296 image

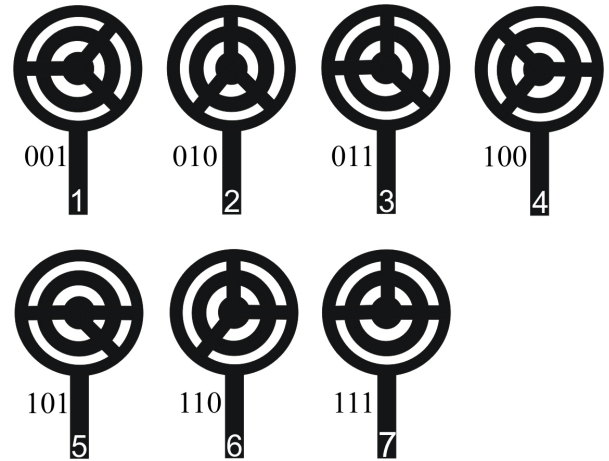


Fig. 1. IDs of LARICS markers

and 3 m distance from the ceiling requires the outer circle radius of 15 cm. The radius of the inner circle is 10 cm.

The coding lines define a 3-bit marker ID that could be used to define path sequences for the mobile robot. For example, path sequence 1-2-3-4-5-6-7-6-5-4-3-2-1 defines a path from the marker with ID 1 to the marker with ID 7 and back. By comparing already passed marker IDs with the predefined sequences, it is easy to localize a mobile platform and conclude if the executed path corresponds to the predefined one. The other benefit is that various paths can be defined without any changes in the marker layout.

## 3. IMAGE PROCESSING ALGORITHM - HOUGH TRANSFORMATION

The Hough transformation [Duda and Hart, 1972] is an image processing method which can be used to isolate features of a particular shape within an image. This method is most commonly used for the detection of curves such as lines, circles, ellipses, etc. It requires specifications of desired shapes in some parametric form.

A circle with radius  $R$  and center  $(a, b)$  can be described with parametric equations:

$$x = a + R \cdot \cos(\phi) \quad (1)$$

$$y = b + R \cdot \sin(\phi) \quad (2)$$

Each point in a geometric space generates a circle in the parameters space. In case the geometric space points belong to the same circle, the center of this circle will be represented by intersection of circles in the parameters space as shown in (Fig. 2).

If radius  $R$  is eliminated from equations (1) and (2) Hough transformation algorithm for circle fitting can be described by equation:

$$b = a \cdot \tan(\phi) - x \cdot \tan(\phi) + y \quad (3)$$

The Hough transform works by letting each point  $(x, y)$  in the geometric space to vote for point  $(a, b)$  in the parameters space for each possible line passing through it. These votes are summed in an accumulator  $M(a, b)$ . If a position  $(a, b)$  in the accumulator has maximum votes,

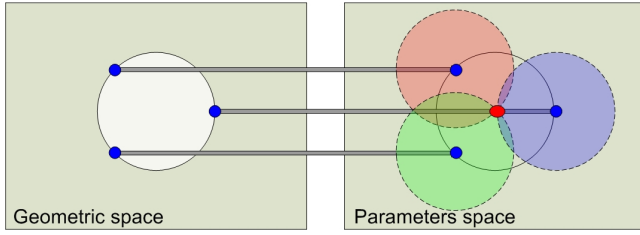


Fig. 2. The Hough transformation idea

this means that position  $(a,b)$  is the center of the circle in the geometric space. To take advantage of this property LARICS markers contain two concentric circles to provide better voting.

In order to be able to extract circles from captured images, an edge detection algorithm should be executed. The Sobel filter is an edge detector whose results yield the magnitude and direction of edges by applying the horizontal and vertical line enhancement mask given below [R. Harley, 2003].

$$G_H = \begin{bmatrix} -1 & -2 & -1 \\ 0 & 0 & 0 \\ 1 & 2 & 1 \end{bmatrix}, G_V = \begin{bmatrix} -1 & 0 & 1 \\ -2 & 0 & 2 \\ -1 & 0 & 1 \end{bmatrix} \quad (4)$$

Edge magnitude and phase are given by:

$$G_{SOBEL} = \sqrt{G_H^2 + G_V^2} \quad (5)$$

$$\theta_{SOBEL} = \tan^{-1} \left( \frac{G_V}{G_H} \right) \quad (6)$$

Now the circle fitting algorithm can be described as follows:

- Create parameter space  $M(a,b)=\{0\}$
- Calculate image gradient magnitude  $G(x,y)$  and angle  $\theta(x,y)$
- Calculate equation (3) on each edge point with magnitude  $G(x,y)$  above threshold, (parameter  $a$  is unknown, it can be limited if circle radius is known)
- Local maxima in  $M(a,b)$  correspond to circles centers within an image

An image captured by on-board camera converted to grey scale is shown in Fig. 3. The result of Hugh transformation of image in Fig. 3 is given in Fig. 4 and Fig. 5. It can be clearly seen that the maximum value in the parametric space  $M(a,b)$  is achieved in the marker center. As already said, the voting process is improved by using two concentric circles.

#### 4. MARKER INFORMATION EXTRACTION

As mentioned before, LARICS fiducial markers provide information about the position (provided by the marker center), orientation (determined by the orientation line) and marker (defined by the coding lines). As the first step in marker information extraction, a gray area around the marker is converted to black and white. The size of the area to be converted is obtained by using the distance to the ceiling and the real size of the marker (Fig. 6). Each pixel in that area is converted to black or white depending on its intensity (with respect to a predefined threshold). Due to

Fig. 3. Captured marker image

Fig. 4. The Hough transformation result, 2D view of  $M(a,b)$

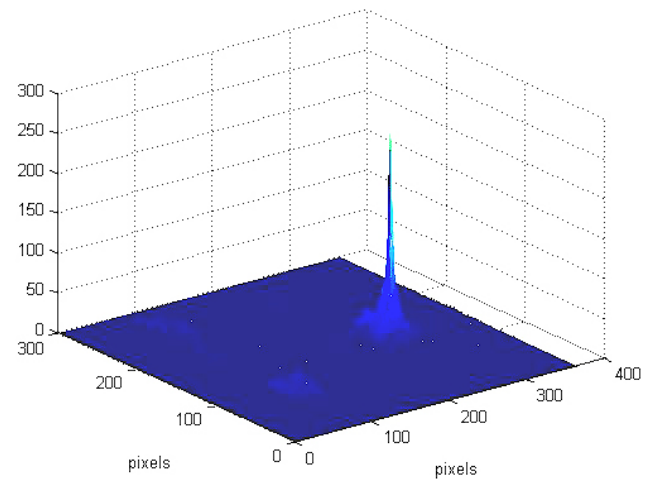


Fig. 5. The Hough transformation result, 3D view of  $M(a,b)$

Fig. 6. Marker information extraction

varying light conditions the adaptive threshold algorithm is used.

Once the black and white area is obtained, marker information extraction starts from the center of marker.

Let  $\alpha$  be an angle and  $r$  radius of a particular point (in b-w area) in the polar coordinate system with intensity  $I(\alpha, r) = \{0, 1\}$ , where 0 represents a black pixel and 1 represents a white pixel. Then, the algorithm for orientation line detection is defined as:

$$H(\alpha) = \sum_{r=0}^{r=N} \bar{I}(\alpha, r), \forall \alpha \in \{0, 359\} \quad (7)$$

Equation (7) is calculated for each angle from  $0^\circ$  to  $359^\circ$  (in counterclockwise direction), and for each radius from the 0 to  $N$ , where  $N$  represents a distance (in pixels) from marker center. The value of parameter  $N$  must be large enough to include the whole marker. Accounting the predefined resolution of 2 pixel/cm at  $360 \times 296$  image, 3 m ceiling distance, 8 cm orientational line length and marker outer circle radius of 8 cm, a value of  $N=32$  pixels has been calculated using equation (8):

$$N = res * (r + l) \quad (8)$$

where  $res$  [pix/cm] is marker resolution at image,  $r$  [cm] is outer circle radius and  $l$  [cm] is length of orientation line.

The equation (7) sums black pixels for every angle  $\alpha$  on the line defined with  $r$ . The result,  $H(\alpha)$ , is shown in Fig. 7. The highest value of  $H(\alpha)$  represents the orientation line angle which, in our example, corresponds to  $35^\circ$  shift from the zero angle (Fig. 7a). The orientation line angle is defined as *transient zero angle* and all coding lines are defined with respect to this angle.

Once the orientation line (transient zero angle) has been determined, for every  $45^\circ$  portion from the transient zero angle (the angle between coding lines is  $45^\circ$ , see Fig. 1), the average value  $Z$  is calculated as:

$$Z = (\sum_{n=1}^7 H(45 * n)) / 6 \quad (9)$$

The variable  $Z$  is used as a threshold for identification of coding lines (Fig. 7c).

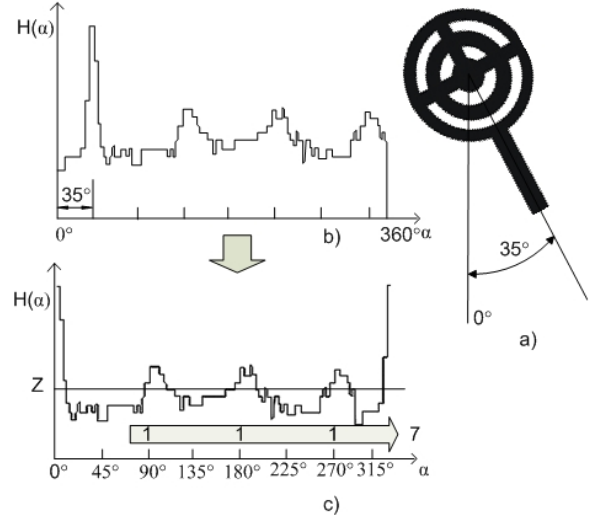


Fig. 7. Function  $H(\alpha)$  for marker ID 7

As defined, coding lines shifted for  $90^\circ$ ,  $180^\circ$  and  $270^\circ$  from the transient zero angle. Hence, in case  $H(90^\circ) > Z$ , MSB in ID is 1, for  $H(180^\circ) > Z$ , center bit is 1, and for  $H(270^\circ) > Z$ , LSB in ID is 1. In example shown in (Fig. 7c), all three values of  $H(\alpha)$  that correspond to the coding lines are above  $Z$ , therefore the algorithm identifies marker ID 7.

## 5. PRACTICAL IMPLEMENTATION AND EXPERIMENTAL RESULTS

A practical implementation of visual feedback indoor control system based on markers has been successfully tested on mobile platform SHREC. The markers have been placed on the ceiling and simple tracking algorithms have been implemented to provide marker path tracking.

Usually, camera calibration is an essential preliminary step in solving complicated image analysis tasks. However, due to the fact that the influence of distortion on a circular shape is negligible, in our application image processing has been done with an uncalibrated camera.

The second issue that should be taken into account is ambient light intensity. In order to capture an image with good contrast value, the light intensity should be above certain level. Absence of light could decrease the probability of marker detection. The other problem related to light is a change in light intensity that could be caused by lamps on the ceiling. Although most webcams provide automatic brightness adjustment, the adaptation time could be significant. On average, a web camera needs 6 frames for successful brightness adjustment. This means that the proposed marker detection algorithm must wait for 2-3 seconds before a new image with good quality is obtained. As a solution, an extra light source from a lamp mounted on top of the robot can be used. Better camera, or camera driver with high speed auto-brightness could improve performance as well.

A practical implementation of the visual feedback indoor control system has been tested on LARICS testing field (Fig. 8). The field contains 3 markers that are facing each other. A simple tracking algorithm has been imple-

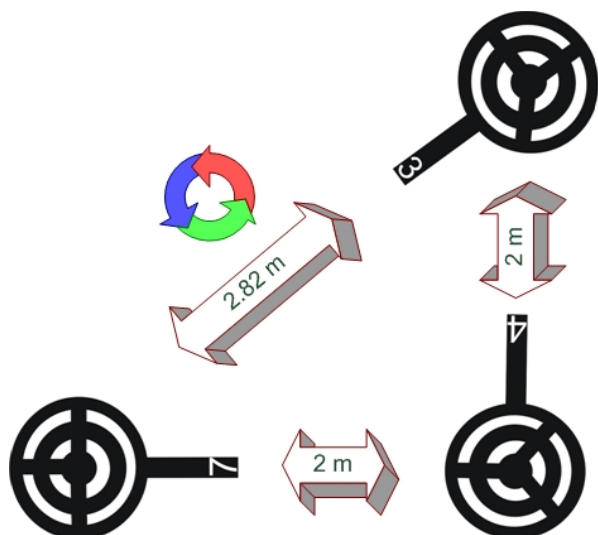


Fig. 8. LARICS testing field

mented for path tracking. Firstly, we have investigated the influence of ambient light on marker detection, and secondly, proposed marker detection algorithm sensitivity with respect to mobile robot speed (motion blur effect).

Tables 1-3. show results of our marker detection algorithm while the robot was moving from one marker to the other in counterclockwise direction.

In Table 1. results obtained in case of low intensity of ambient light are shown. During a 7 minute time period, 1186 frames were captured and in 630 images marker was detected (due to the camera angle and distance between markers, approximately 50% of images contained markers - images taken when mobile platform was located between markers did not include a marker). A total of 8% of detected markers were interpreted incorrectly. Table 2. shows results obtained on a sunny day. During 7 minutes, markers have been detected in 772 images, and only 4% of detected markers were interpreted incorrectly. Due to better ambient light number of detected markers (772) increased 18% with respect to the case when ambient light was insufficient (630). Nominal testing speed of mobile platform was 20 cm/s. Results shown in Table 3. have been obtained with increased speed (twice the normal speed) on a sunny day. It can be seen that 7% of markers have been interpreted incorrectly. The influence of motion blur effect is approximately the same as influence of low ambient light. The sensitivity to motion blur could be reduced by slowing down the platform as it approaches the expected marker position.

Table 1. Cloudy day, ambient light influence test

Marker ID	3,4 and 7	Other
Marker detection	92%	8%

Table 2. Sunny day, ambient light influence test, normal speed

Marker ID	3,4 and 7	Other
Marker detection	96%	4%

Fig. 9 shows screenshots of moving platform with captured images (upper left corner). When a marker is detected, the

Fig. 9. Larics testing field, marker approaching algorithm

algorithm controls platform in order to set a marker in the center of captured image (images 1 and 2). Once in the center, platform heading is aligned with the orientation line of the marker (image 3) and robot proceeds towards the next marker (image 4).

Table 3. Sunny day, light influence test, double speed

Marker ID	3,4 and 7	Other
Marker detection	93%	7%



## 6. CONCLUSION

This paper presents a simple fiducial marker design that can be easily detected by low cost web camera using an embedded microcomputer system with limited capabilities. Marker design is very important in improving detection and reducing computational time. We have chosen a circular shape to provide more robust localization information. Furthermore, the fiducial marker is based on two circles, one inside the other in order to improve marker detection. Experimental results have confirmed that low ambient light intensity, as well as increased mobile platform speed, did not considerably influence marker detection probability. Future work will be devoted to the improvement of marker detection capabilities in case of significant change in light conditions with markers positioned on the floor and/or on the shelves in a store. Finally, proposed system shall be implemented on a autonomous cleaning machine and tested under realistic operating conditions.

*robot localization and mapping with uncertainty using scale-invariant visual landmarks*, pages 735–758, 2002.

## REFERENCES

- R.K. Harle A.C. Rice, A.R.Beresford. Cantag: an open source software toolkit for designing and deploying marker-based vision systems. *Pervasive Computing and Communications*, 2006., 2006.
- Robert K. Harle Andrew C. Rice and Alastair R. Beresford. Analysing fundamental properties of marker-based vision system design. *Pervasive and Mobile Computing* 2, pages 125–247, 2006.
- S.T. Birchfield Chen Zhichao. Qualitative vision-based mobile robot navigation. *Robotics and Automation*, 2006. *ICRA 2006. Proceedings 2006 IEEE International Conference*, pages 2686– 2692, 2006.
- Richard O. Duda and Peter E. Hart. Use of the hough transformation to detect lines and curves in pictures. *Communications of the Association of Computing Machinery* 15, pages 11– 15, 1972.
- Wonpil Yum Jaeyeong Lee Heesung Chae and Young-Jo Cho. Robot localization sensor for development of wireless location sensing network. *Intelligent Robots and System, 2006 IEEE/RSJ International Conference*, pages 37–42, 2006. doi: <http://dx.doi.org/10.1016/j.robot.2006.11.001>.
- S. Kim K. Yoon, G. Jang and I. Kweon. Fast landmark tracking and localization algorithm for mobile self-localization. *IFAC Workshop on Mobile Robot Technology*, pages 190–195, 2001.
- card by K-TEAM S.A. KoreBot. Yverdon-les-bains. 2007.
- R. Weeks Arthur R. Harley, R. Weeks Myler. *The Pocket Handbook of Image Processing Algorithms in C*. Department of Electrical & Computer Engineering University of Central Florida, Orlando, Florida, 2003.
- J. Rekimoto and Y. Ayatsuka. Cybercode: Designing augmented reality environments with visual tags, 2000. URL [citeseer.ist.psu.edu/rekimoto00cybercode.html](http://citeseer.ist.psu.edu/rekimoto00cybercode.html).
- R. Setola G. Ulivi S. Panziery, F. Passuci. A low cost vision based localization system for mobile robots. *In 9th Mediterranean Conf. on Control and Automation, Dubrovnik, Croatia.*, 2001.
- J. Little S. Se, D. Lowe. Robust self-localization of mobile robots using artificial and natural landmarks. *Mobile*